



Temporal downscaling of precipitation time-series projections to forecast green roofs future detention performance

Vincent Pons^{1,2}, Rasmus Benestad³, Edvard Siversten⁴, Tone Merete Muthanna¹, and Jean-Luc Bertrand-Krajewski²

¹Department of Civil and Environmental Engineering, The Norwegian University of Science and Technology, Trondheim, 7031, Norway

²Univ Lyon, INSA Lyon, DEEP, EA7429, 11 rue de la Physique, F-69621, Villeurbanne cedex, France

³Norwegian Meteorological Institute, Oslo, Norway

⁴SINTEF AS, S.P. Andersens veg 3, N-7465 Trondheim, Norway

Correspondence: Vincent Pons (vincent.pons@ntnu.no)

Abstract. A strategy to simulate rainfall by the means of different Multiplicative random Cascades (MRC) was developed to evaluate their applicability to produce inputs for green roof infrastructures models taking into account climate change. The MRC reproduce a (multi)fractal distribution of precipitation through an iterative and multiplicative random process. The initial model was improved with a temperature dependency and an additional function to improve its capability to reproduce the temporal structure of rainfall. The structure of the models with depth and temperature dependency was found to be applicable in eight locations studied across Norway (N) and France (F). The resulting time-series from both reference period and projection based on RCP 8.5 were applied to two green roofs (GR) with different properties. The different models lead to a slight change in the performance of GR, but this was not significant compared to the range of outcomes due to ensemble uncertainty in climate modelling and the stochastic uncertainty due to nature of the process. The moderating effect of the green infrastructure was found to decrease in most of the Norwegian cities, especially Bergen (N), while increasing in Lyon (F).

1 Introduction

Hydrologic performance of stormwater Green Infrastructure (GI) is usually divided between Retention and Detention. Retention refers to water stored, infiltrated, or evapotranspired. Actual evapotranspiration can be estimated from a water balance including Potential Evapotranspiration, accumulated precipitation, a soil moisture evaluation function, a, and, a crop factor (Johannessen et al., 2017; Oudin et al., 2005). Evapotranspiration process time-scale is typically 24 hours or less. Detention refers to water temporarily stored in the GI before being discharged into a downstream stormwater network. The process time-scale is typically a few minutes. Consequently, modelling GI detention performance requires higher resolution data to estimate its outflow (Schilling, 1991). Therefore, both high resolution climate data and projections at sub daily and sub hourly scales are needed in order to model GIs, and to estimate their potential as a climate change adaptation measure.

In Norway and most of the European countries, precipitation has been measured with tipping buckets in numerous cities from years to decades. Moreover, climate projection for future precipitation and temperature from the EURO-CORDEX project are



available at 1*1 km spatial resolution in Norway (Dyrrdal et al., 2018) and 12*12 km resolution in France (Jacob et al., 2014). Consequently, the use of such data by urban hydrologists to assess the resilience of GI solutions to face climate change is conditioned by the possibility to downscale them to a sub-hourly resolution.

25 Downscaling includes two families of methods: Dynamical downscaling and Statistical downscaling (Benestad, 2016). Dynamical downscaling methods use physically based equations and are usually very computationally expensive specially to obtain high resolution data. Statistical downscaling consists in improving the resolution of data based on statistical properties observed on a lower resolution dataset. Its computational cost is lower. Therefore, statistical methods might still be used to fill the gap in the next decades until the computational power is high enough to use accurate enough physically based models.

30 Statistical downscaling has already been extensively used to temporally downscale data to various resolutions, usually hourly or daily data. Three popular methods can be mentioned: *i*) the method of fragment, *ii*) the method based on point process theory, and *iii*) the method of multiplicative random cascades. The method of fragment (Li et al., 2018; Lu et al., 2015) is a resampling method based on k-nearest neighbours (Kalra and Ahmad, 2011), which has been applied to derive hourly data from daily data. It can be accurate and effective thanks to its resampling nature, but it requires a large dataset, and by its design cannot ensure
35 extrapolation from observed data. Therefore, it might not be suitable to downscale climate projections. Methods based on point process theory have been used (Glasbey et al., 1995; Onof et al., 2000). The main principle is to generate storm occurrences and then describe them based on rain cells and statistical distribution based on Poisson point process . Multiplicative random cascades (MRC) consist of using successively random cascades to split data in N data of finer resolution ($N = 2$ in most of the cases). It is a very popular method that deserves further investigations (Gaur and Lacasse, 2018; Rupp et al., 2012; Thober
40 et al., 2014). Multiplicative random cascades can be divided between canonical and micro-canonical types. The canonical MRC is often calibrated by fitting to the curve of non-centred moments of depths or intensity through time-scale (Paschalis et al., 2012) and typically does not conserve exactly the volume. The principle of micro-canonical MRC is usually based on reverse cascades: studying how the data are split and then reproducing the properties of the weights distribution depending on different quantities. The influences of time-scale, rainfall intensity (Paschalis et al., 2012; Rupp et al., 2009) or season (McIntyre et al.,
45 2016) have been extensively studied. Lombardo et al. (2012) Lombardo et al. (2012) suggested the commonly used MRC suffers from conceptual weaknesses due to the non-stationary process of autocorrelation and proposed a method to improve the model. More recently, (Bürger et al., 2014, 2019) suggested to include a temperature dependency in MRC models to make them more robust. This enables them to be used with projections.

While downscaling model have been used to model the performance of green infrastructure under current climate (Stovin
50 et al., 2017), or applied to IDF curves in order to do an event based simulation of local stormwater measures (Kristvik et al., 2019), none has been developed to produce future high resolution time-series as input for green infrastructure model. The aim of this research is to evaluate different MRC downscaling models and for their potential to produce input time-series to predict the performance of stormwater green infrastructure, for the case of green roofs. In order to achieve this aim, different parts are detailed in the paper: *i*) the development of a general structure of MC; *ii*) the improvement of this MC structure by adding a
55 temperature dependency , *iii*) the addition of an ordering function to improve the temporal structure of the produced rainfall



time-series; *iv*) the evaluation of the capability to reproduce the performance of GI based on observed data; and finally *v*) the analysis of the possible shift in performance of GI at the end of the century.

2 Methods

2.1 Meteorological data

60 Time-series of precipitation and temperature from six locations in Norway and two in France, representing four different climates (Table 1) according to the Köppen Geiger classification (Peel et al., 2007), were used to apply the downscaling method. In Norway, the precipitation was measured by 0.2 mm Plumatic Kongsberg tipping rain gauges. The rain gauges were not heated and thus did not operate in cold temperature. They were successively replaced to Lambrecht 1518H3 (measuring range of 0.1mm) in the 1990s and 2000s. The stations were operated by the Norwegian Water Resources and Energy Directorate
 65 (NVE) and the Norwegian Meteorological institute (MET). The data were quality checked by the Norwegian Meteorological institute (MET) (Lutz et al., 2020). In Lyon, precipitation was measured by 0.2 mm Précis-Mécanique tipping bucket rain gauges. Ten climate projections (temperature and precipitation) on daily resolution with the RCP 8.5 for the period from 2071 to 2099 for Norwegian cities were available online <https://nedlasting.nve.no/klimadata/kss> (Dyrrdal et al., 2018). For Lyon and Marseille (France), twelve climate projections were available from <http://www.drias-climat.fr/>.

70 2.2 Downscaling models and workflow

2.2.1 Data aggregation and processing

The data were aggregated two by two from 1-minute resolution (resp. 6-minute) to more than 1-day resolution in order to capture a part of the uncertainty linked to the estimation of the parameter of the models . The aggregation was done for each possible time-steps: all multiple of 2 smaller than 1500 min. During the process of aggregation, both the weights (1) and the
 75 temporal coherence indicator S (2) measuring the proportion of high weight on the side of the highest neighbouring depth w were computed. Given i a time-step, j a temporal resolution in minutes, and d a rainfall depth, the weight w and the indicator S of the side of the neighbour were calculated according to:

$$w_{i,2j} = \frac{\min(d_{2i,j}, d_{2i+1,j})}{d_{2i,j} + d_{2i+1,j}} \in [0; 0.5] \quad (1)$$

$$80 \quad S_{i,2j} = \begin{cases} 0, & \text{if } (d_{i-1,2j} = d_{i+1,2j}) \cup (d_{2i,j} = d_{2i+1,j}) \\ 1, & \text{if } (d_{2i,j} > d_{2i+1,j} \cap d_{i-1,2j} > d_{i+1,2j}) \cup (d_{2i,j} < d_{2i+1,j} \cap d_{i-1,2j} < d_{i+1,2j}) \\ 2, & \text{if } (d_{2i,j} > d_{2i+1,j} \cap d_{i-1,2j} < d_{i+1,2j}) \cup (d_{2i,j} < d_{2i+1,j} \cap d_{i-1,2j} > d_{i+1,2j}) \end{cases} \quad (2)$$



Table 1. Locations and input data; Climate column gives the Köppen Geiger classification for climate, Ndays is the number of days with simultaneously data of precipitation and temperature (it includes dry days), All cities except Bron are located in Norway

Location	Climate	Latitude	Precipitation data	Temperature data	Ndays
Bergen – Sandsli, MET 50480, NVE no. 56.1.	Cfb	60.4	[1984 – 2020], R=0.1 mm	[1989-2020]	6150
Bodø – Skivika, MET 82310, NVE no. 165.11.	Dfc	67.3	[1997 – Nov. 2004], R=0.2 mm [Nov. 2004 - 2020], R=0.1mm	[1997-2020]	7204
Lyon (France), 6-min time-step	Cfb	45.7	[1992 – 2012], R=0.1 mm 6-min time-step	[1992-2012] daily time-step	7671
Hamar – Hamar II (Disen), MET 12290	Dfb	60.8	[1968 – 2008], R=0.2 mm [2008 – 2020], R=0.1 mm	[2008-2020]	4011
Kristiansand – Sømkleiva, MET 39150, NVE no. 21.49.	Cfb	58.1	[1974 – 2004], R=0.2 mm [2004 – 2020], R=0.1 mm	[1999-2020]	5219
Kristiansund – Karihola, MET 64300, NVE no. 110.1.	Cfb	63.1	[1974 – 2006], R=0.2 mm [2006 – 2020], R=0.1 mm	[1987 – 2020]	8664
Marseille (France), 6-min time-step	Csa	43.3	[1990 – 2009], R=0.1 mm 6-min time-step	[1990 – 2009] daily time-step	7305
Trondheim – Risvollan, MET 68230, NVE 123.38.	Dfc	63.4	[1986 – 2020], R=0.1mm	[1986 – 2020]	10722

2.2.2 Downscaling process

The downscaling process consists of transforming daily rainfall depths to rainfall depths at shorter time-steps, e.g. one minute, by means of successive children time-steps which are half of the parent time-steps. Three probability functions were used to achieve the downscaling process. The probability to have a weight equal to zero (3) represents the probability to assign all the water from the parent time-step to only one of the children time-steps. This property is especially important and acknowledged by other studies. The distribution on non-zero weights (4), modelled with a truncated normal distribution rescaled on [0,0.5], was used after the zero-weight step. It was chosen against more commonly used beta distributions (McIntyre et al., 2016) after a goodness of fit test. The last function (5) is associated to the rainfall continuity indicator S and represents the probability to place the highest weight on the side of the highest neighbour (i.e. allocating rain to a children time-step to the nearby parent



90 time-step which the highest rain):

$$P(W = 0), \text{ with } W \in [0; 0.5] \quad (3)$$

$$P(W = w | W \neq 0), \text{ with } w \in [0; 0.5] \text{ and } W \sim \mathcal{N}(0.5, 1, [0; 0.5]) \quad (4)$$

95 $P(S = 1), \text{ with } S \in \{0; 1\} \quad (5)$

The MRC models were developed to ensure a parsimonious number of parameters. Homogeneity of the resolution in the input datasets was not required for calibration and data processing (i.e. the model can be calibrated using multiple datasets with different resolutions between 1-min and 1 day). The modelled properties were time-scale continuous to allow the model to be used with all initial resolution smaller 1500 min. Based on the observed data, the functions were chosen to represent equations 3, 4 and 5, depending on the variable. Figure 1 describes the downscaling process. The models MCS, MCDS and MCDTS (Table 2) all included 5 (indicated with S), while the MC, MDS, and MCDT model considered equal probability (0.5) to have a weight on one side or the other. MCD and MCDS model included a depth (D) dependency when generating the occurrence of the zero-weight, MCDT and MCDTS model included both depth and temperature (DT) at this step. In practice, the downscaling started at 1440 min (1 day) time-step with 8 iterations to reach a time-step of 5.625 min. The results were then interpolated and scaled to a 6-min time-step for comparison with observed data. The final time-step of 6 minutes was chosen based on the resolution of original datasets in Lyon and Marseille.

Table 2. The various quantities taken into account by each model depending on the process considered; R is the time-scale, D the rainfall depth, T the temperature and N the close neighbour.

Model	$P(W = 0)$				$CDF(W, W \neq 0)$				$P(S_w = high)$				Number of parameters
	R	D	T	N	R	D	T	N	R	D	T	N	
1-MC	x			x									8
2-MCS	x			x				x			x		13
3-MCD	x	x		x									14
4-MCDS	x	x		x				x			x		19
5-MCDT	x	x	x	x									13
6-MCDTS	x	x	x	x				x			x		18

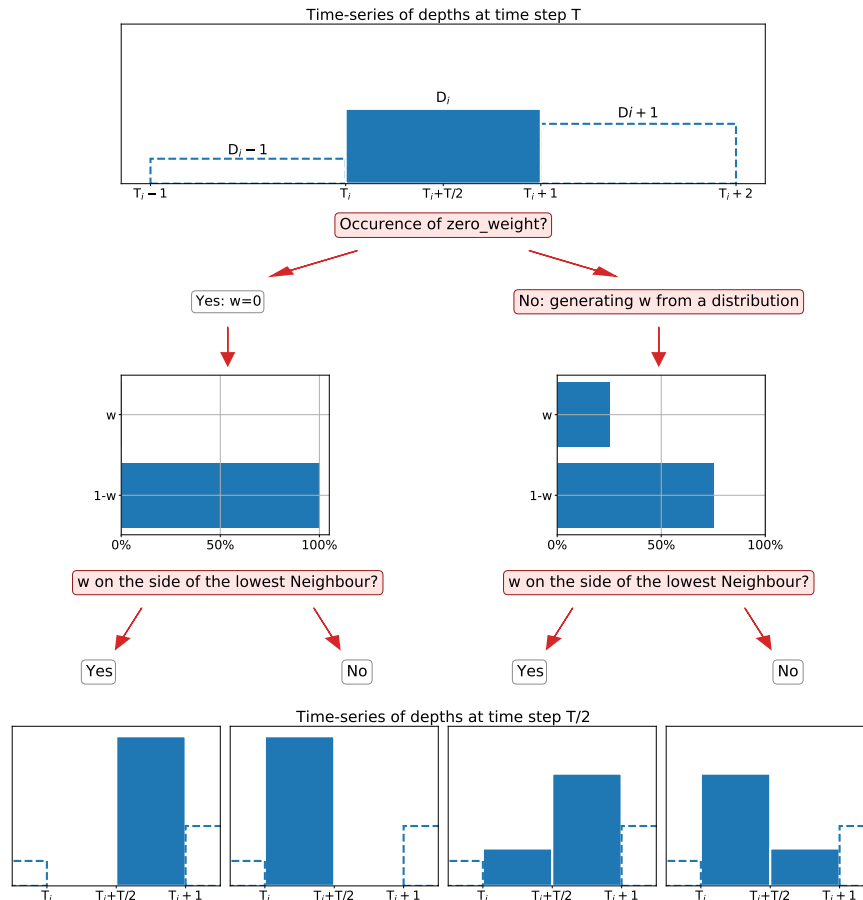


Figure 1. Workflow for downscaling to transfer a depth from time-step T to time-step $\frac{T}{2}$. The red boxes involve the generation of a random number. The process starts with 1440 minute time-step to reach 5.625 min an interpolation is then done to reach 6 min time-step.

2.3 Green Infrastructure modelling

In order to quantify the influence of rainfall input in green roof performance estimation, two green roofs located in Trondheim were modelled: *i*) A typical extensive green roof (E-green roof) with sedum vegetation, 30 mm of substrate, and 10 mm of “eggbox” drainage layer (Hamouz and Muthanna, 2019), and *ii*) a detention-based extensive green roof (D-green roof) with sedum vegetation, 30 mm of substrate, and 100 mm of lightweight clay aggregates (Hamouz et al., 2020). The model is a simple reservoir model with differentiable linear function (8) for the outflow, Oudin’s model for Potential Evapotranspiration (PET) and a Soil Moisture Evaluation Function (SMEF) to estimate Actual Evapotranspiration (AET) (Johannessen et al., 2017).

$$WC_i = WC_{i-1} + P_{i-1} - Q_{i-1} - WC_{i-1} \times PET_i \times C \quad (6)$$



115

$$PET_i = \begin{cases} 0, & \text{if } T_i \leq 5^\circ\text{C} \\ \frac{Ra}{\lambda\rho} \times 0.01 \times (T_{mean} + 5), & \text{if } T_i > 5^\circ\text{C} \end{cases} \quad (7)$$

$$Q_i = \begin{cases} \frac{S_K}{1 + \exp(-\frac{4 \times K}{S_K} \times (WC_i - WC_K - \frac{S_K - 1}{2 \times K}))}, & \text{if } WC_i > WC_K + \frac{S_K - 1}{2 \times K} \\ K \times (WC_i - WC_K) + \frac{1}{2}, & \text{else} \end{cases} \quad (8)$$

WC_i is the water content (mm) at time t_i . P_i is the precipitation ($\text{mm} \cdot \text{min}^{-1}$). The discharge Q_i ($\text{mm} \cdot \text{min}^{-1}$) is based on the empirical curve (8). The temperature T_{mean} is in Celsius degree, the extra-terrestrial radiation Ra is derived from the latitude and the Julian day. The constant $\frac{1}{\lambda\rho} \approx 0.408$ depends on latent heat and volumetric mass of water. The factor C is a calibrated factor depending on the maximum storage and the crop factor. The smoothed linear curve (8) with K the conductivity slope, S_K the smoothing factor and WC_K the starting delay. The model was developed based on data from extreme tests with artificial precipitation (Hamouz et al., 2020) by establishing a relationship between water content and runoff. One day of data collected during extreme tests including nearly dry roof, successive artificial rainfall events leading to saturation and drainage of the roof during twelve hours. The relative water content was computed based on inflow and outflow and shifted to ensure positive water content. The outflow depending on water content was used as input for calibration of the discharge function using Bayesian calibration with DREAM setup (Laloy and Vrugt, 2012). The D-green roof's model was validated with a rainfall series of two and half month from July 2018 to the 25th of September, and a one-month series from the 5th of September 2019 to the 5th of October. The E-green roof's model was validated with a rainfall series from April 2017 to September 2017. Snow periods were mostly excluded for the evaluation.

2.4 Evaluating the downscaled time-series

For each location, the observed precipitations were aggregated to daily resolution and downscaled to obtain 200 time-series of 6-min time-step. They were used to model all the extensive and detention-based extensive green roofs in parallel. It should be noted that irrigation needs, and snow periods were neglected since the primary objective of the study was to evaluate the produced time-series. There are 10 projections available in Norway for the RCP8.5 and 12 in France with the EURO-Cordex project. Each projected time-series was downscaled 20 times (200 simulations for Norwegian locations, and 240 simulations for French locations) to capture: *i*) the variability between the projections and *ii*) the variability due to the nature of the downscaling model. The number of simulations per location and per period was chosen to ensure reasonably low simulation time and represent the stochastic uncertainty inherent to the downscaling process. The stability of the percentile estimator with 200 simulations was verified against 1000 simulations in one model and one location to validate the choice.

To evaluate the performance of the downscaling model and the projected performance of green roofs, different indicators were used:



- 145
- The lag-1 autocorrelation depending on time-step. It was chosen to assess the temporal structure of the produced time-series.
 - The survival distribution of precipitation and of discharge from both roofs at 6-min time-step. This approach was similar to the use of flow duration curves recently applied to green roofs by Johannessen et al. (2018). The exceedance probabilities were presented with a log axis to account for extreme probabilities. The median, 5th and 95th percentile of the downscaled time-series were represented. The survival distribution of discharge from the roofs with downscaled
 - 150 time-series compared to the distribution based on observed data indicates the applicability of the downscaled time-series as an input for green infrastructure modelling.
 - Three different discharge thresholds were used to report exceedance frequency on different operating modes: 1L/s/ha for small events, 10 L/s/ha for major events and 100L/s/ha for extreme events.
 - The distribution of dry periods and the retention fraction. They are not expected to be affected by the downscaling
 - 155 process since the dry periods affecting the roofs can be observed on daily resolution, and the retention fraction can be estimated with conceptual models using daily time-step data. However, they provide additional information to analyse the behaviour of the roofs.

3 Result and discussion

3.1 Green infrastructure model

160 The parametrized empirical reservoir model was applied to the extensive green roof and the detention-based extensive green roof. The performance was evaluated both on the time-series and individual events extracted from the time-series. The criteria were: *i*) Nash Sutcliffe Efficiency (*NSE*) indicator on time-series for both discharge and water content, *ii*) *NSE* for rainfall events defined with a minimum inter events time of 6-hours to analyse further the behaviour of the model, and *iii*) the volumetric error on the time-series to account for model retention evaluation. The observed water content was estimated directly from

165 discharge measurement using the empirical curve. The performance was as follow:

- $NSE > 0.8$ for both discharge and water content for the extensive green roof. On the 3 most intense events the *NSE* ranged from 0.9 to 0.75. The water balance error was found to be 2.1%.
- $NSE > 0.94$ for both discharge and water content for the detention-based extensive roof. On the 3 most intense events the *NSE* ranged from 0.96 to 0.85. The water balance error was found to be 5%.

170 The model is limited as it lumped processes and neglects dynamical effect: the wetting of the aggregates and substrate and the spatial distribution of water content within the roof (Hamouz et al., 2020). It can be seen in Figure 2 in the beginning of the events. It suggests that short events with low intensity are not reproduced well by the model as it cannot represent the delay induced by the wetting of the different layers of the roofs. Since the objectives of this study involve the use of a simple model to reproduce the behaviour of two roofs, the model was not further improved.

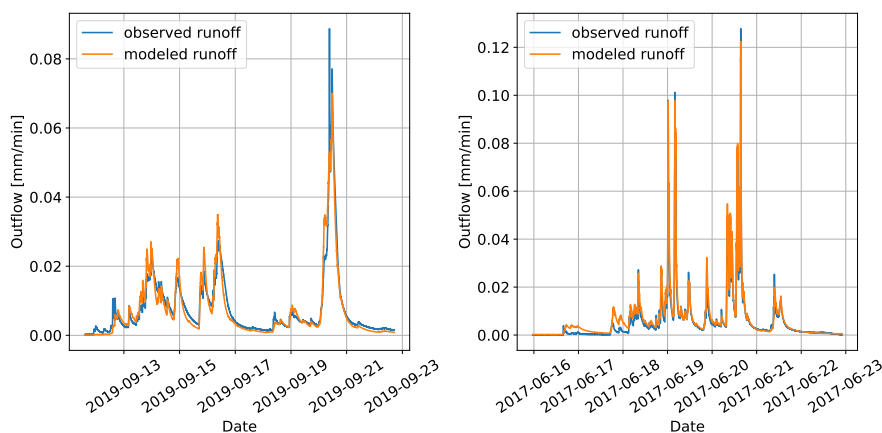


Figure 2. Validation of the green roof's reservoir model. Observed and modelled runoff of the detention-based extensive green roof (D) model on ten days period (left) and extensive green roof (E) for a period of eight days (right) in Trondheim.

175 3.2 Analysis of climates properties

Figure 3 presents the zero-weight proportion depending on time-scale, depth and temperature for two different datasets (Bodø and Hamar). On Figure 3a the proportion of zero-weight decrease with increasing time-scale for Bodø. In Hamar the proportion decrease until 45 min and increase for higher time-scale. Based on this observation, two types of datasets were identified in terms of zero-weight occurrence. For data from Bodø, Bergen, Kristiansund and Trondheim, the proportion of weights that equalled zero decreased with increasing time-scale. For the data from Hamar, Bron and Kristiansand, the proportion that decreased until 45 minutes time-scale and increased afterward. Given a time-scale, the proportion of weight equal to zero was not uniform depending on the weights (e.g. Bodø and Hamar Figure 3b lower left plot with a time-scale of 48 minutes). Therefore, the monotony or non-monotony of the proportion of weights equalling to zero depending on time-scale can be explained by different distribution of depth in the observed data. The proportion depended on depth, which is consistent with previous work (Rupp et al., 2009).

In Figure 3b, the zero-weights proportion decreases with increasing depth for the case of Bodø. In the case of Hamar, it increases for depth higher than 2 mm. The two plots on the right show that a temperature dependency may explain this behaviour. In Bodø, the proportion depending on depth gives similar results for different ranges of temperature at 48-min resolution. On the contrary, in Hamar, the subsets with lower temperature lead to a lower proportion of weights being equal to zero, compared to subsets with higher temperature. Moreover, the higher depths were observed in subsets with higher temperature. The increase observed in Hamar can be explained by the distribution of observed values. It is consistent with the observation of different temporal distributions of rainfall for different temperature ranges such as convective rain (Berg et al., 2013; Zhang et al., 2013). If, given a depth of 10 mm at resolution of 48 minutes, the probability to have a weight equal to zero is higher, then there is a higher probability to have an intense rainfall. The non-homogeneity of observed datasets and



195 the shift in temperature with climate change might lead to inconsistency in datasets produced by the downscaling methods
 that exclude depth and/or temperature dependency. Developing a simple model is easy but might prevent comparability of
 parameters between locations and does not necessarily lead to parameter parsimonious models. Moreover, a model such as
 MCD can result in overfitting when used with datasets like Hamar. The functions necessary to represent the behaviour without
 considering the temperature dependency are more complex and less explanatory. Adding the temperature dependency could
 200 result in a more explanatory model with more robust results for the influence of climate change.

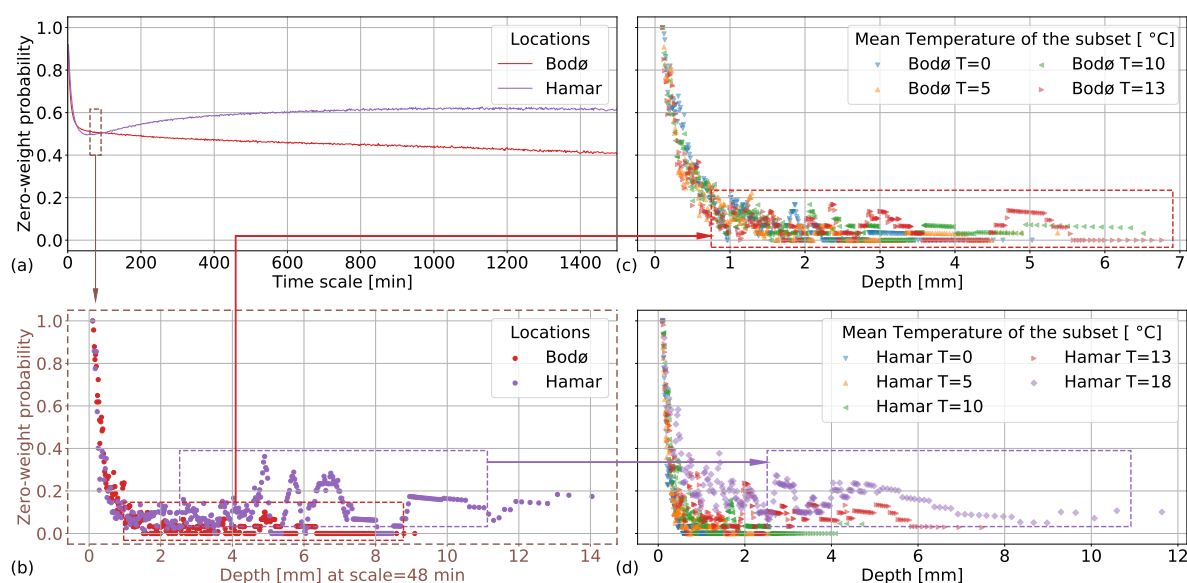


Figure 3. Dependency of the probability to have a weight equal to zero on, time-step (a), rainfall depth (b) and temperature (c and d) for datasets observed in Bodø and Hamar. b, c, and d are based on data at 48-minutes resolution.

3.3 Evaluation of the downscaling methods

An overview of the performance of the downscaling and green roof models in Bergen is presented on Figure 4. All the downscaling models performed similarly in terms of dry period distribution and slightly underestimate the dry periods in observed data (Figure 4b). The dry periods were directly linked to the zero-weight probability. In green infrastructure modelling, length
 205 of the dry periods influences the retention performance as it can lead to water stress hindering evapotranspiration. However, dry periods leading to water stress can be also evaluated with daily time-step series (there is no need for minute time-step series). Therefore, dry periods longer than the initial daily resolution are not significantly affected by downscaling.

The distribution of precipitation (Figure 4a) was properly reproduced by the MCD, MCDS, MCDT, and MCDTS models while the MC and MCS underestimated low precipitation and overestimated high precipitation depth. This was expected as
 210 the time-steps with high depth have higher probability to not be split in the observed data. It is not the case for the MC and



MCS models, where the probability is uniformly distributed. In Bergen, the observed precipitations were contained within the range of 90% coverage interval for the MCD, MCDS, MCDT, and MCDTS. The discharge was slightly underestimated (Figure 4c,d). However, it was not the case for all locations, as in Hamar the most extreme precipitations tended to be underestimated while the discharge from both roofs had the same order of magnitude as the observed data but tended to be overestimated. 215 These findings could suggest inconsistency in the temporal structure of rainfall. This hypothesis can be confirmed by the autocorrelation (Figure 4e) being overestimated at 6 minutes time-step. The autocorrelation was underestimated in the MC and MCS model. The use of the rainfall continuity indicator in the models increased the autocorrelation for all models but did not improve the overall performances.

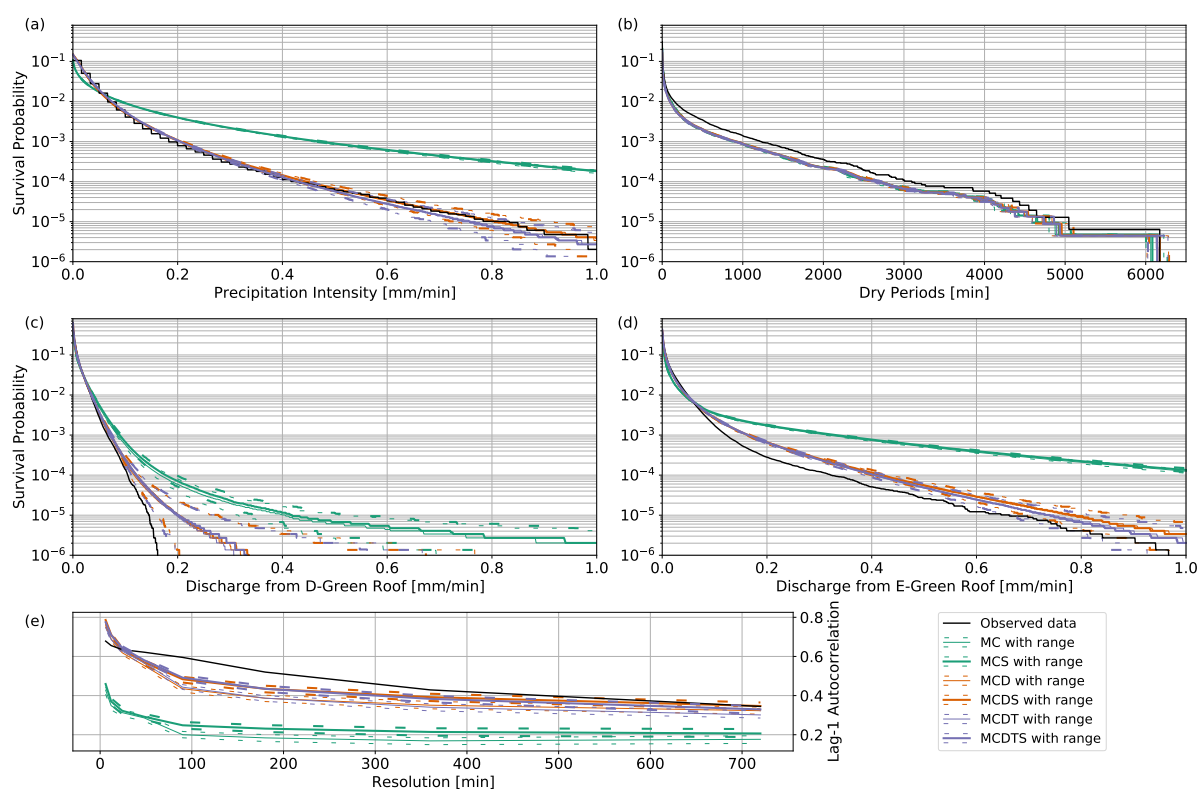


Figure 4. Models performance with data from Bergen's current climate for the MC, MCS, MCD, MCDS, MCDT and MCDTS with a range from the 5th to 95th percentile.

To evaluate the produced time-series it is necessary to compare the discharge with observed time-series to the discharge with downscaled time-series. For most of the location, the predicted range of precipitation or discharge deviated for lowest 220 probabilities from the values obtained with observed time-series: *i*) When the precipitation range match with the observed distribution, the discharge tended to be overestimated; *ii*) When the precipitation was underestimated, the discharge with observed data tends to lay in the range obtained from downscaled time-series. The performance based on downscaled time-



series might lead to biased result if used as a discharge from observed time-series. Moreover, the raw discharge time-series
225 might not be suitable for robust decision making in green infrastructure implementation as it does not represent the natural
variation of performance of green infrastructure.

In order to evaluate the potential of discharge from downscaled time-series to approach the range of performance linked
to natural variability, a 3-year moving window was used on precipitation time-series and discharge time-series resulting from
observed precipitation. The resulting 5th and 95th percentile of the annual time exceeding 1L/s/ha, 10L/s/ha and 100L/s/ha
230 is presented in Figure 5 to evaluate the time-series in different operating modes of the roofs. It is compared to the stochastic
variability (5th and 95th percentile) from the 6 models. Each horizontal line in Figure 5 represents the range between the 5th
and 95th percentile for the threshold and model considered. The different thresholds represent respectively discharge for small
events, for major events and extreme events. On Figure 4, the threshold corresponds to 0.006 mm/min, 0.06 mm/min and 0.6
mm/min. A good estimate is defined by a complete or partial overlap between the observed natural variability and the stochastic
235 variability range conserving the order of magnitude of the range. For instance, in Bergen, the observed range of the D-green
roof higher than 10L/s/ha is 9 to 16 hours so less than a day; the MC model provide a range from 24 to 28 hours, more than
a day it is not a good estimate as there is no overlap and the order of magnitude change; the MCD model result in a range
from 14 to 17 hours. It is a good estimate as the range are overlapping, and the order of magnitude is similar. The MC and
MCS models tend to underestimate the order of magnitude of the range of exceedance frequencies of the small events (1L/s/ha)
240 (in Bergen Hamar and Marseille) but tend to overestimate major (10L/s/ha) (Hamar) and extreme events (100L/s/ha) (Bergen
Bodø Hamar and Marseille). The other models gave mostly good estimates for each of the thresholds (Figure 5, Figure A1).
In Marseille, the models MCD, MCDS, MCDT and MCDTS tended to underestimate the higher bound of the extreme event
precipitation with values lower than 50 minute per year whereas the observed time-series led to a maximum of 90 minutes per
year. However, those models kept the order of magnitude, while model MC and MCS estimated it higher than 10^2 minutes. The
245 same behaviour was observed with Hamar (Figure 5) and Lyon datasets (appendix, Figure A1). This suggests that the models
performed worse with dryer location, possibly due to the calibration procedure since less wet days are available for calibration.
The models MCD and MCDT performed similarly, but due to its structure, MCD risks to overfit to the calibration data. It could
result in an inaccurate prediction in case of significant temperature shift between the calibration and prediction datasets. To
conclude the model MC and MCS lead to overestimation of the natural variability range; the model MCD MCDS MCDT and
250 MCDTS gives more accurate estimates.

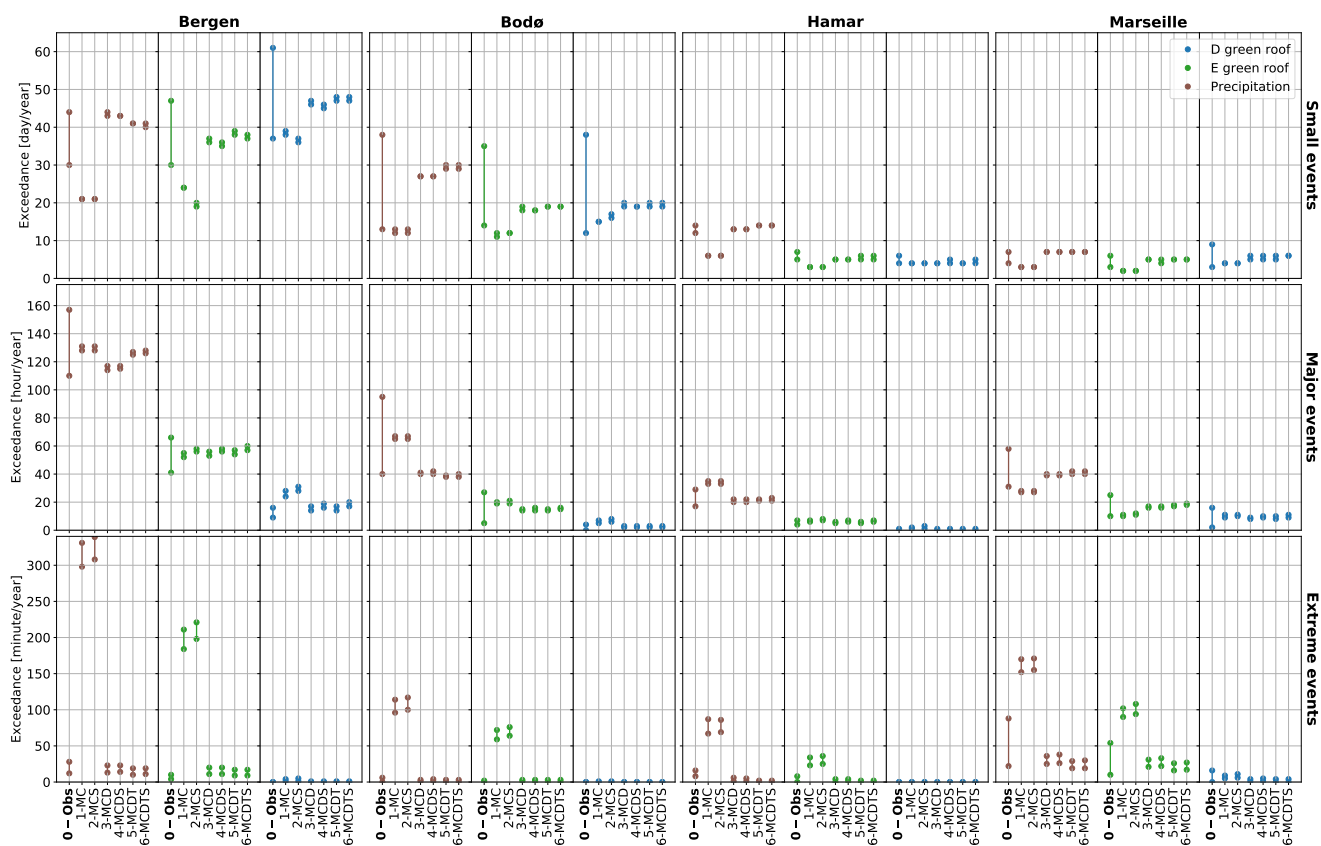


Figure 5. Performance of the downscaled time-series in Bergen, Bodø, Hamar and Marseille, the exceedance frequency is in day/year for small events, hour/year for major events and minute/year for extreme events. the model 0-Obs result of the observed precipitation time-series with a 3-year moving window to estimate the 5th and 95th percentile.



3.4 Assessment of green roof future performance

All six models were used to assess the future performance of green roofs for future climate as illustrated for Bergen in Figure 6. It was nevertheless acknowledged that MC and MCS models gave less accurate estimates. The four model MCD MCDS MCDT and MCDTS lead to similar results in Bergen (Figure 6). The difference in estimates between the models with coherence indicator (MCDS, MCDTS) and without (MCD, MCDT) was negligible in comparison to the stochastic uncertainty inherent to the models and the variability linked to the different projections available under RCP8.5 (Figure 6). In Bergen, according to the projections, the performance of the two solutions is likely to lead to worse performance: under current climate, the 100 L/s/ha exceedance was lower than 1 minute for the D-green roof; according to the MCDTS model it might reach between 5 and 19 minutes in future climate. It suggested a shift in the order or magnitude from 10^0 to more than 10^1 minutes. Similarly, the E-green roof might have a 100 L/s/ha exceedance shift from 10^1 to 10^2 minutes. It means that the threshold would regularly be reached.

As illustrated by Figure 7 and Figure A2, the performance shift depends highly on the location. The 100L/s/ha exceedance of the green roofs was likely to get worse in Bergen, to stay stable despite a small increase in Bodø and to improve in Hamar and Marseille. The increase of exceedance frequency in the Norwegian cities was due to an increase in precipitation. However, the increase in temperature led to an increase in potential evapotranspiration and therefore might have attenuated or even counterbalanced the effect of rainfall increase by lowering the initial water content in the roofs at the beginning of a rainfall event. The Table 3 shows that the retention fraction was likely to decrease in Bergen, Bodø, Hamar, Kristiansand and Kristiansund. It was found to increase in Lyon, Marseille and slightly in Trondheim. The models with temperature dependency performed similarly to the model with only depth dependency in most of the location. However, in Lyon and Marseille, the 100 L/s/ha exceedance or precipitation predicted differed from 16-27 min to 21-50 min (resp. 14-30 to 14-43 in Marseille). This suggests that some locations are more sensitive than other to temperature dependent patterns. The models MCD, MCDS MCDT and MCDTS allow to evaluate shift in performance for the different roofs using exceedance range.

Table 3. Retention fraction in the different locations defined as the sum of outflow divided by the sum of precipitation.

Location	Bergen		Bodø		Lyon		Hamar	
Period	Observed	Projected	Observed	Projected	Observed	Projected	Observed	Projected
D-Green roof	0.20	0.17	0.21	0.20	0.43	0.47	0.47	0.40
E-Green roof	0.19	0.16	0.21	0.20	0.39	0.44	0.44	0.38
Location	Kristiansand		Kristiansund		Trondheim		Marseille	
Period	Observed	Projected	Observed	Projected	Observed	Projected	Observed	Projected
D-Green roof	0.24	0.22	0.25	0.20	0.27	0.30	0.41	0.47
E-Green roof	0.22	0.20	0.24	0.20	0.26	0.29	0.36	0.42

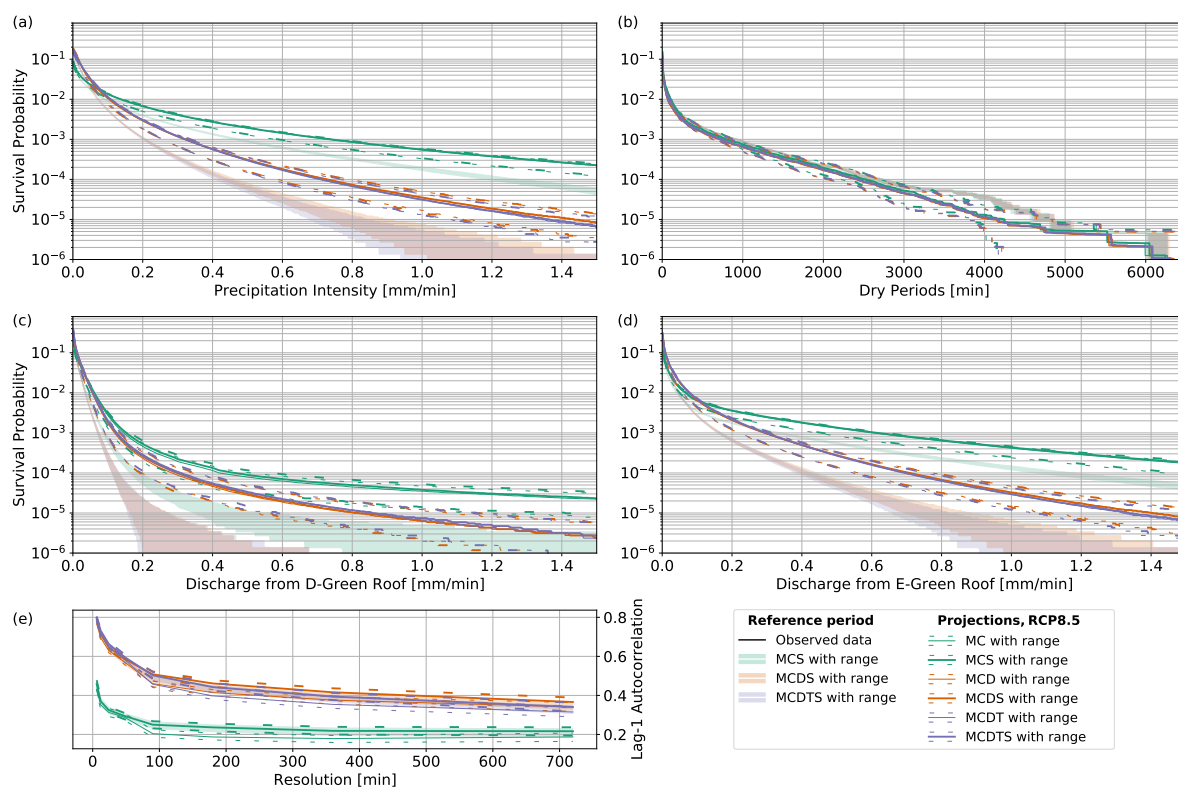


Figure 6. Comparison between performance under current climate and future climate in Bergen for the MC, MCS, MCD, MCDS, MCDT and MCDTS with a range from the 5th to 95th percentile.

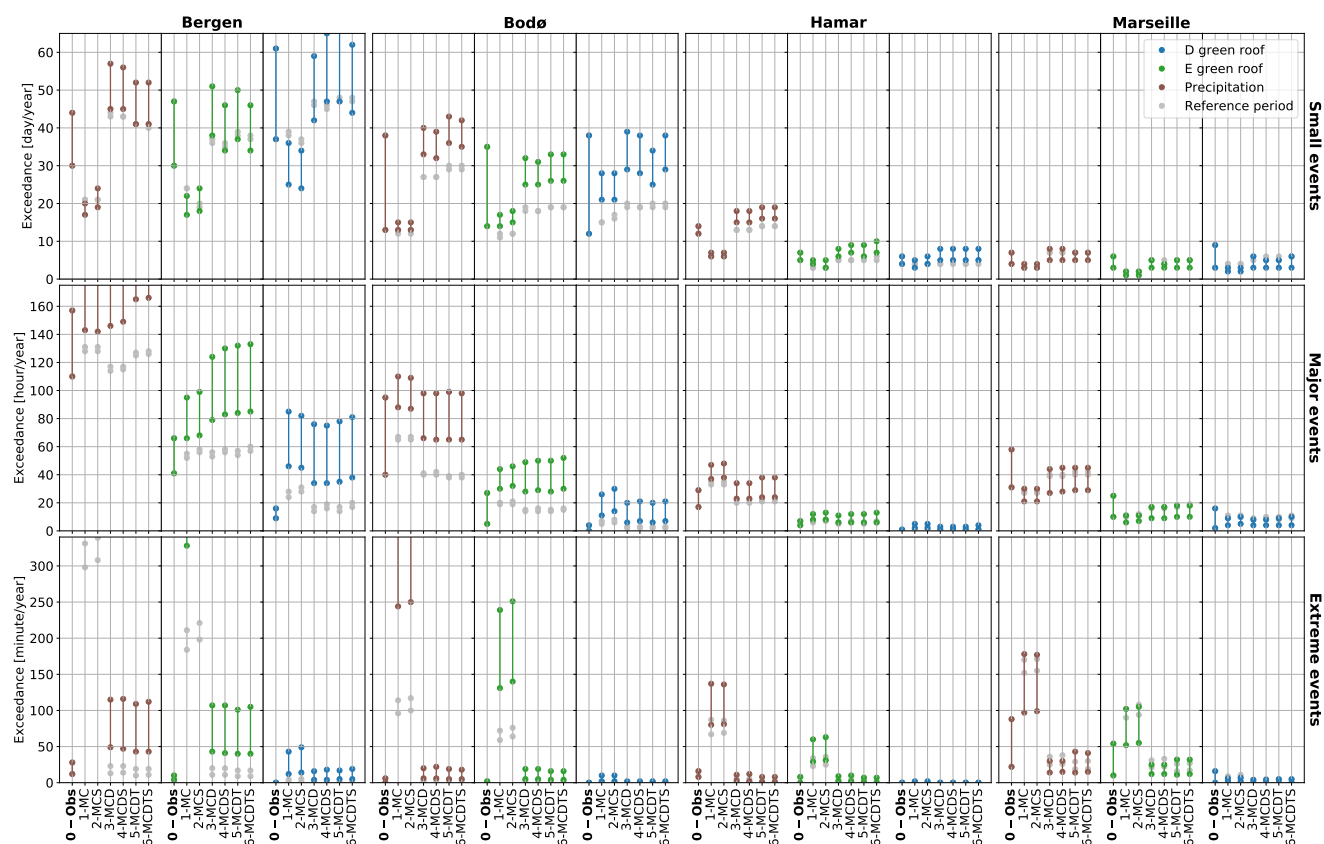


Figure 7. Future performance of green roofs (D and E) in Bergen, Bodø, Hamar and Marseille representing the 4 different climates modelled. The exceedance frequency is in day/year for small events, hour/year for major events and minute/year for extreme events. the model 0-Obs result of the observed precipitation time-series with a 3-year moving window to estimate the 5th and 95th percentile.



3.5 Design perspectives

In order to conclude on the applicability of downscaled time-series to predict the future performance of green infrastructure, the methods were compared to the current recommended practice in Norway: the use of the variational method (Alfieri et al., 2008) with the use of a climate factors (CF)(Kristvik et al., 2019; Trondheim Kommune, 2015). The results presented, for the city of Trondheim and 2, 5 and 10-year return period rainfall and runoff events, include: *i*) peaks runoff of runoff events based on an observed precipitation time-series, *ii*) the peak runoff or rainfall events based on variational method with and without climate factor and, *iii*) an hybrid approach based on downscaling 10^5 rainfall events with a daily depth based on to the return period curves with and without climate factors (Figure 8). This last approach used the MCDTS model. According to the current recommendation in Norway for Trondheim municipality, a climate factor of 1.4 was applied (Dyrødal and Førland, 2019). The figure shows that the variational method underestimated the peaks runoff with observed data, and the distribution from the hybrid approach covered them. It suggests that the variational method might not be enough conservative when compared to peak runoff from runoff events instead of rainfall events. Even if the results from the hybrid event-based downscaling lead to realistic distribution based on probable rainfall events, the downscaling models might need a different calibration or conceptualization to be optimized specifically for extreme events. The observed peaks show a range of possible outcome which highlight the limitations of the variational method with a single estimate, whereas the hybrid downscaling-event based method, leading to a range of probable outcomes, gave promising results that can lead to more robust design and decision making.

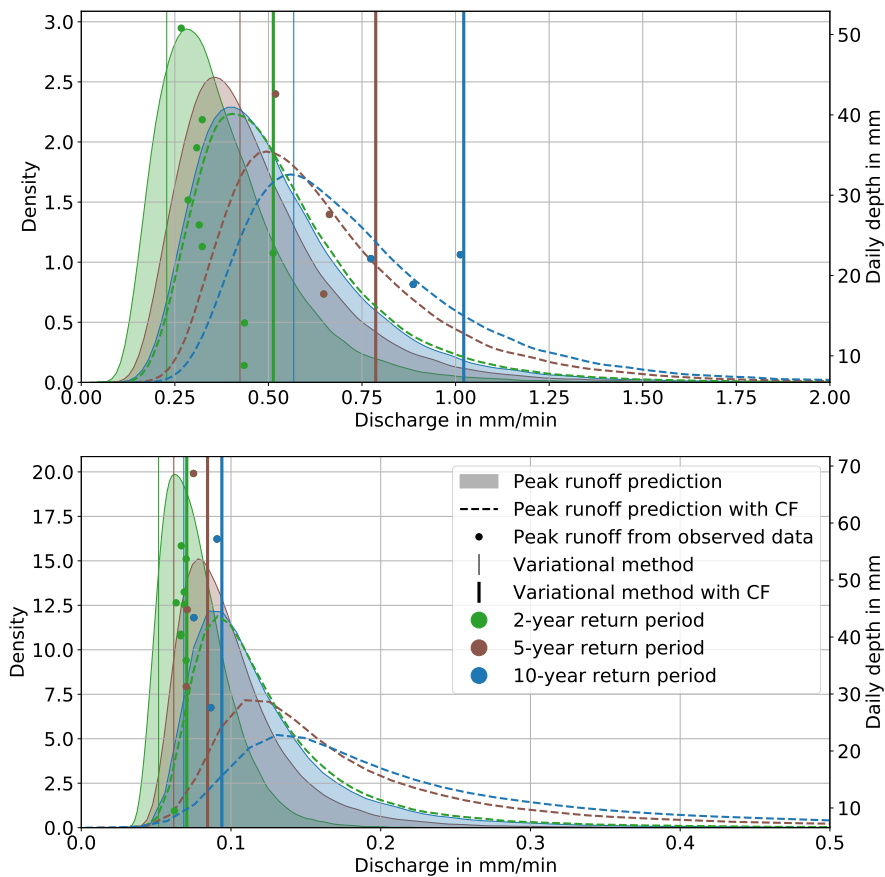


Figure 8. Performance depending on the return period in Trondheim for the extensive green roof (top) and the detention-based extensive green roof (bottom). The transparent coloured area (resp. dotted line) is the distribution based on the hybrid event-based downscaling under current climate (resp. with CF); the points represent the peaks runoff of runoff events from observed precipitation; the vertical lines the results found based on the VM. 2, 5 and 10-year return period are displayed.



4 Conclusions

290 In this study, multiplicative random cascades models with different variable dependency were developed. They were based on a study of time-scale, depth, and temperature characteristics of the datasets to ensure a consistent structure in the view to apply them to daily resolution climate projections. The applicability of the synthetic time-series to be used as input for performance modelling of green infrastructure was evaluated. They were used to predict the shift in runoff exceedance under a future climate.

295 Six downscaling model were developed: two models with only time-scale dependency (MC and MCS), two models with time-scale and depth dependency (MCD and MCDS) and two models with time-scale, depth and temperature dependency (MCDT and MCDTS). The models MCS, MCDS and MCDTS include a rainfall continuity property with the intention to improve the temporal structure of the rainfall. The parametrization of the models ensures the continuity of the different properties modelled and a low number of parameters.

300 The MC and MCS were not sufficient to predict the future performance of green infrastructure as they lead to overestimation of runoff; The MCD, MCDS MCDT and MCDTS lead to better performance: it was possible to predict runoff exceedance frequency with similar order of magnitude to an estimate of the natural variability of performance based on observed time-series. The structure of the MCD and MCDS models make them more vulnerable to overfitting than MCDT and MCDTS which make them less reliable for future performance estimate. However, the differences between them were negligible compared to
305 the variability linked to the different outcome of climate models, the variability inherent to the model and its accuracy. The MCS, MCDS and MCDTS add an equation to improve the temporal structure of downscaled rainfall. The models predicted higher runoff from the detention-based extensive green roof, which is consistent with their properties, however the change in performance was not significant compared to stochastic uncertainty.

Using the RCP8.5, the different downscaling and green roof models suggests that the shift in performance due to climate
310 change highly depends on the location. The runoff exceedance is likely to increase in Bergen while decrease in Lyon and Marseille and keeping the same order of magnitude in the other locations. The results were compared to one of the current practices: the use of the variational method with a climate factor. It highlighted the limitation of this practice that provide a singular estimate and underestimate the observed peaks. A hybrid method using downscaling on extreme events led to promising results by estimating a distribution of performance of peak runoff.

315 The models performed well in the 8 locations and 4 different climates. The use of a more advanced calibration procedure with Bayesian methods should improve the results. Similarly, a sensitivity analysis could improve the parametrization, especially for the models with depth and temperature dependency in order to fix non behavioural parameters. The current study does not include irrigation and snow modelling a study centred on green infrastructure modelling is therefore needed to extend the results. In order to be applied in practice on event-based simulation for design perspectives, the downscaling models needs to
320 be improved with a calibration procedure developed for extreme events and not on the complete spectrum of observation as in the current study.



Appendix A

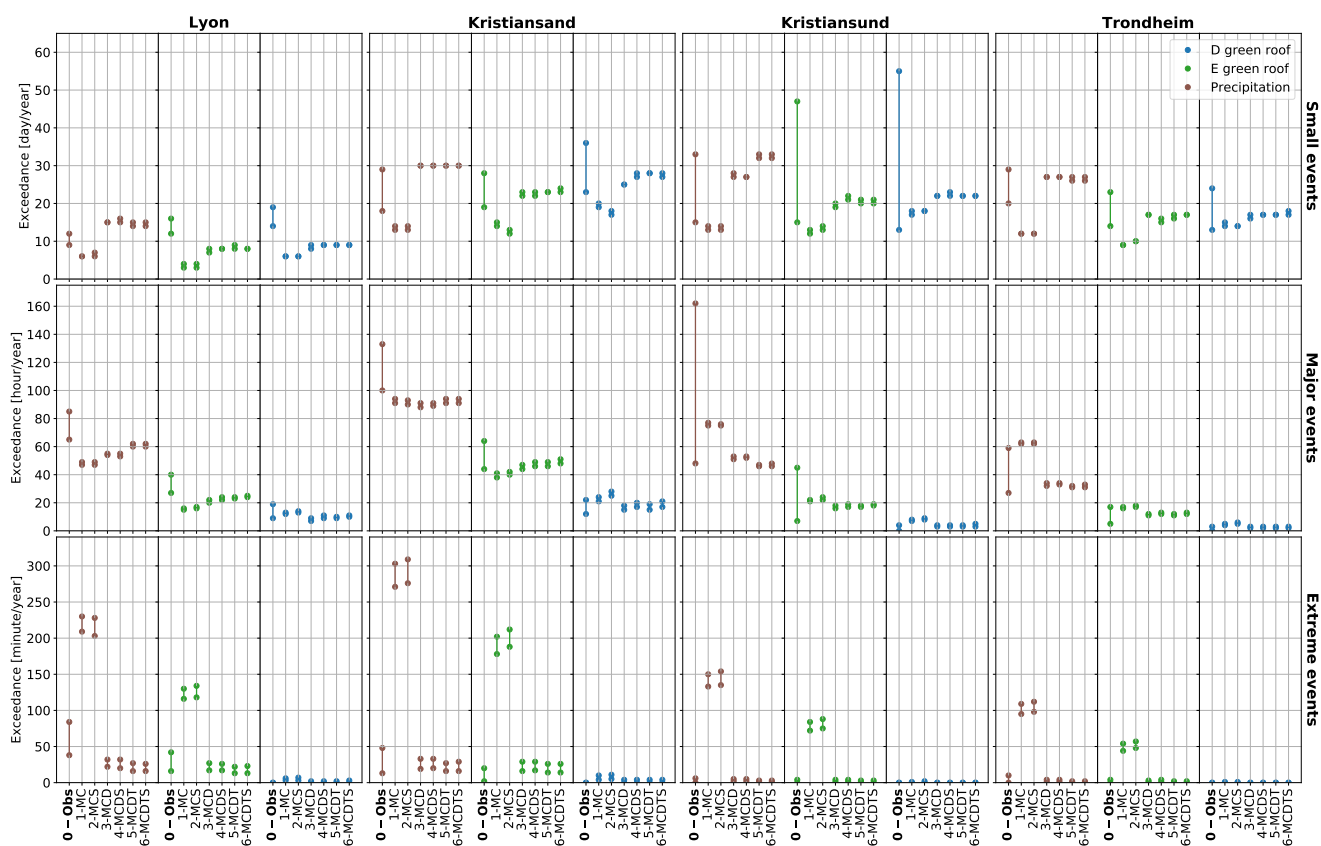


Figure A1. Performance of the downscaled time-series in Lyon, Kristiansand, Kristiansund and Trondheim. The exceedance frequency is in day/year for small events, hour/year for major events and minute/year for extreme events. The model 0-Obs result of the observed precipitation time-series with a 3-year moving window to estimate the 5th and 95th percentile.

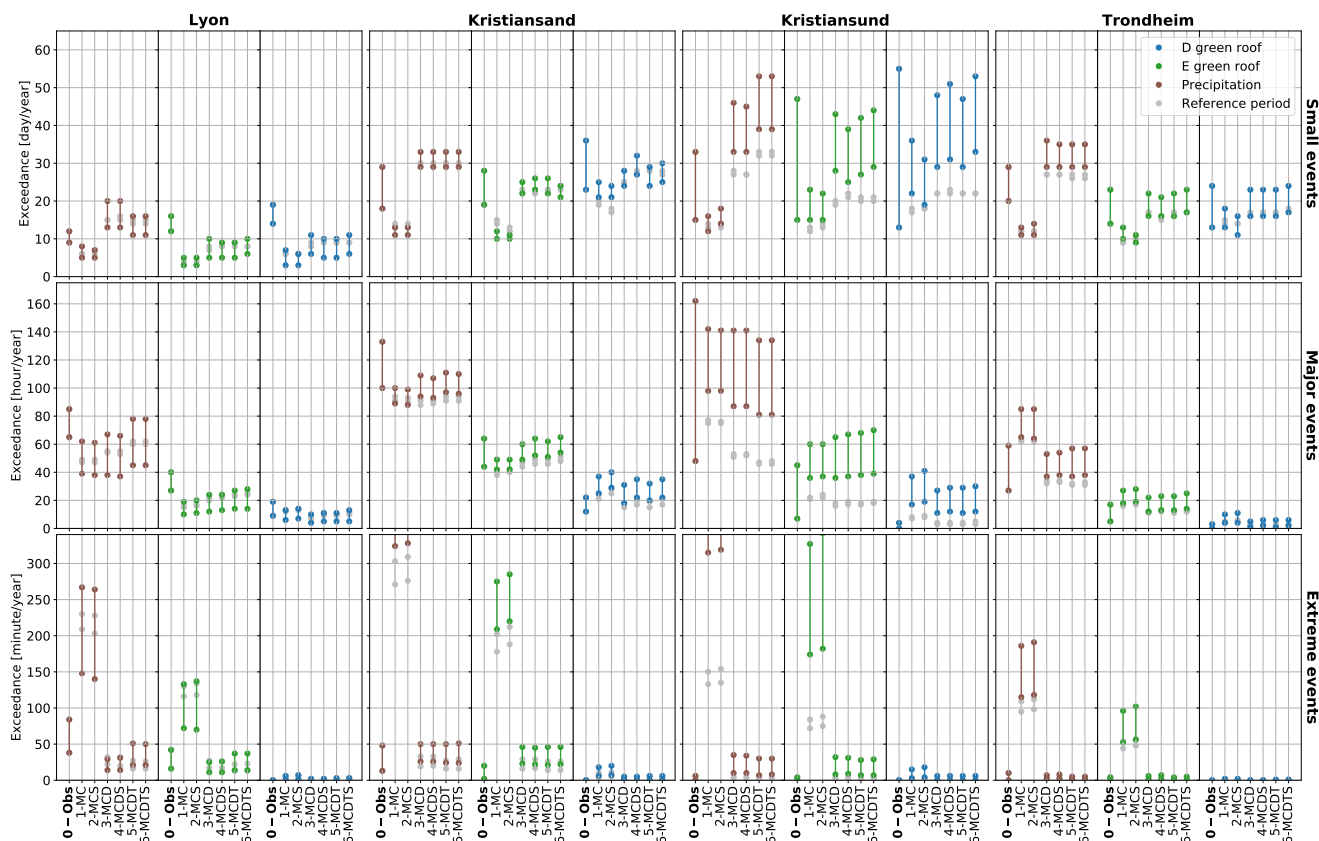


Figure A2. Future performance of green roofs (D and E) in Lyon, Kristiansand, Kristiansund and Trondheim. The exceedance frequency is in day/year for small events, hour/year for major events and minute/year for extreme events. the model 0-Obs result of the observed precipitation time-series with a 3-year moving window to estimate the 5th and 95th percentile.



Author contributions. Vincent was responsible for developing and programming the downscaling and green roofs models. Rasmus provided his expertise in downscaling. Jean-Luc came up with the idea of comparison with the variational method. The Norwegian meteorological institute, represented by Rasmus provided the Norwegian data, Jean-Luc provided the French data. Tone, Edvard and Jean-Luc supervised each step of the study. Vincent wrote the first manuscript. The manuscript was revised by all co-author.

Competing interests. The authors declare that they have no competing interests

Acknowledgements. The study was supported by the Klima2050 Centre for Research-based Innovation (SFI) and financed by the Research Council of Norway and its consortium partners (grant number 237859/030). The authors acknowledge the Water Department of Lyon Metropole and the Water and Sewerage Department of Marseille Provence Metropole for sharing their rainfall data. The authors would like to thank the Norwegian Meteorological institute for providing the norwegian data and especially Cristian Lussana and Lars Grinde for their advices.



References

- Alfieri, L., Laio, F., and Claps, P.: A simulation experiment for optimal design hyetograph selection, *Hydrological Processes: An International Journal*, 22, 813–820, 2008.
- Benestad, R.: Downscaling Climate Information, in: *Oxford Research Encyclopedia of Climate Science*, <https://doi.org/10.1093/acrefore/9780190228620.013.27>, 2016.
- Berg, P., Moseley, C., and Haerter, J. O.: Strong increase in convective precipitation in response to higher temperatures, *Nature Geoscience*, 6, 181–185, 2013.
- 340 Bürger, G., Heistermann, M., and Bronstert, A.: Towards subdaily rainfall disaggregation via clausius-clapeyron, *Journal of Hydrometeorology*, <https://doi.org/10.1175/JHM-D-13-0161.1>, 2014.
- Bürger, G., Pfister, A., and Bronstert, A.: Temperature-driven rise in extreme sub-hourly rainfall, *Journal of Climate*, <https://doi.org/10.1175/JCLI-D-19-0136.1>, 2019.
- Dyrddal, A. and Førland, E.: Klimapåslag for korttidsnedbør-Anbefalte verdier for Norge, NCCS report 5, 2019.
- 345 Dyrddal, A. V., Stordal, F., and Lussana, C.: Evaluation of summer precipitation from EURO-CORDEX fine-scale RCM simulations over Norway, *International Journal of Climatology*, <https://doi.org/10.1002/joc.5287>, 2018.
- Gaur, A. and Lacasse, M.: Multisite multivariate disaggregation of climate parameters using multiplicative random cascades, *Urban Climate*, <https://doi.org/10.1016/j.uclim.2018.08.010>, 2018.
- Glasbey, C. A., Cooper, G., and McGechan, M. B.: Disaggregation of daily rainfall by conditional simulation from a point-process model, *Journal of Hydrology*, [https://doi.org/10.1016/0022-1694\(94\)02598-6](https://doi.org/10.1016/0022-1694(94)02598-6), 1995.
- 350 Hamouz, V. and Muthanna, T. M.: Hydrological modelling of green and grey roofs in cold climate with the SWMM model, *Journal of Environmental Management*, 249, 109–350, <https://doi.org/10.1016/j.jenvman.2019.109350>, 2019.
- Hamouz, V., Pons, V., Sivertsen, E., Raspati, G. S., Bertrand-Krajewski, J.-L., and Muthanna, T. M.: Detention-based green roofs for stormwater management under extreme precipitation due to climate change, *Blue-Green Systems*, <https://doi.org/10.2166/bgs.2020.101>, 2020.
- 355 Jacob, D., Petersen, J., Eggert, B., Alias, A., and Christensen, O. B.: EURO-CORDEX: new high-resolution climate change projections for European impact research, *Regional environmental change*, 14, 563—578, 2014.
- Johannessen, B. G., Hanslin, H. M., and Muthanna, T. M.: Green roof performance potential in cold and wet regions, *Ecological Engineering*, <https://doi.org/10.1016/j.ecoleng.2017.06.011>, 2017.
- Johannessen, B. G., Muthanna, T. M., and Braskerud, B. C.: Detention and retention behavior of four extensive green roofs in three Nordic climate zones, *Water*, 10, 671, 2018.
- 360 Kalra, A. and Ahmad, S.: Evaluating changes and estimating seasonal precipitation for the Colorado River Basin using a stochastic nonparametric disaggregation technique, *Water Resources Research*, <https://doi.org/10.1029/2010WR009118>, 2011.
- Kristvik, E., Johannessen, B. G., and Muthanna, T. M.: Temporal downscaling of IDF curves applied to future performance of local stormwater measures, *Sustainability*, 11, 1231, 2019.
- 365 Laloy, E. and Vrugt, J. A.: High-dimensional posterior exploration of hydrologic models using multiple-try DREAM (ZS) and high-performance computing, *Water Resources Research*, <https://doi.org/10.1029/2011WR010608>, 2012.
- Li, X., Meshgi, A., Wang, X., Zhang, J., Tay, S. H. X., Pijcke, G., Manocha, N., Ong, M., Nguyen, M. T., and Babovic, V.: Three resampling approaches based on method of fragments for daily-to-subdaily precipitation disaggregation, *International Journal of Climatology*, <https://doi.org/10.1002/joc.5438>, 2018.



- 370 Lombardo, F., Volpi, E., and Koutsoyiannis, D.: Rainfall downscaling in time: theoretical and empirical comparison between multifractal and Hurst-Kolmogorov discrete random cascades, *Hydrological Sciences Journal*, <https://doi.org/10.1080/02626667.2012.695872>, 2012.
- Lu, Y., Qin, X. S., and Mandapaka, P. V.: A combined weather generator and K-nearest-neighbour approach for assessing climate change impact on regional rainfall extremes, *International Journal of Climatology*, <https://doi.org/10.1002/joc.4301>, 2015.
- Lutz, J., Grinde, L., and Dyrddal, A. V.: Estimating rainfall design values for the City of Oslo, Norway-comparison of methods and quantifi-
375 cation of uncertainty, *Water (Switzerland)*, <https://doi.org/10.3390/W12061735>, 2020.
- McIntyre, N., Shi, M., and Onof, C.: Incorporating parameter dependencies into temporal downscaling of extreme rainfall using a random cascade approach, *Journal of Hydrology*, <https://doi.org/10.1016/j.jhydrol.2016.09.057>, 2016.
- Onof, C., Chandler, R. E., Kakou, A., Northrop, P., Wheeler, H. S., and Isham, V.: Rainfall modelling using poisson-cluster processes: A review of developments, *Stochastic Environmental Research and Risk Assessment*, <https://doi.org/10.1007/s004770000043>, 2000.
- 380 Oudin, L., Hervieu, F., Michel, C., Perrin, C., Andréassian, V., Anctil, F., and Loumagne, C.: Which potential evapotranspiration input for a lumped rainfall-runoff model? Part 2 - Towards a simple and efficient potential evapotranspiration model for rainfall-runoff modelling, *Journal of Hydrology*, <https://doi.org/10.1016/j.jhydrol.2004.08.026>, 2005.
- Paschalis, A., Molnar, P., and Burlando, P.: Temporal dependence structure in weights in a multiplicative cascade model for precipitation, *Water Resources Research*, <https://doi.org/10.1029/2011WR010679>, 2012.
- 385 Peel, M. C., Finlayson, B. L., and McMahon, T. A.: Updated world map of the Köppen-Geiger climate classification, *Hydrology and Earth System Sciences*, <https://doi.org/10.5194/hess-11-1633-2007>, 2007.
- Rupp, D. E., Keim, R. F., Ossiander, M., Brugnach, M., and Selker, J. S.: Time scale and intensity dependency in multiplicative cascades for temporal rainfall disaggregation, *Water Resources Research*, <https://doi.org/10.1029/2008WR007321>, 2009.
- Rupp, D. E., Licznar, P., Adamowski, W., and Léniewski, M.: Multiplicative cascade models for fine spatial downscaling of rainfall: Parameterization with rain gauge data, *Hydrology and Earth System Sciences*, <https://doi.org/10.5194/hess-16-671-2012>, 2012.
- 390 Schilling, W.: Rainfall data for urban hydrology: what do we need?, *Atmospheric Research*, 27, 5–21, [https://doi.org/https://doi.org/10.1016/0169-8095\(91\)90003-F](https://doi.org/https://doi.org/10.1016/0169-8095(91)90003-F), 1991.
- Stovin, V., Vesuviano, G., and De-Ville, S.: Defining green roof detention performance, *Urban Water Journal*, 14, 574–588, 2017.
- Thober, S., Mai, J., Zink, M., and Samaniego, L.: Stochastic temporal disaggregation of monthly precipitation for regional gridded data sets,
395 *Water Resources Research*, <https://doi.org/10.1002/2014WR015930>, 2014.
- Trondheim Kommune: VA-norm. Vedlegg 5. Beregning av overvannsmengde Dimensjonering av ledning og fordøringsvolum [Water and Wastewater Norm. Attachment 5. Calculation of stormwater flows. Design of pipes and detention basins], Tech. rep., The City of Trondheim, <https://www.va-norm.no/trondheim/>, 2015.
- Zhang, Q., Li, J., Singh, V. P., and Xiao, M.: Spatio-temporal relations between temperature and precipitation regimes:
400 Implications for temperature-induced changes in the hydrological cycle, *Global and Planetary Change*, 111, 57–76, <https://doi.org/https://doi.org/10.1016/j.gloplacha.2013.08.012>, 2013.